

The lower cell density of leaf parenchyma in the *Arabidopsis thaliana* mutant *lcd1-1* is associated with increased sensitivity to ozone and virulent *Pseudomonas syringae*

Carina Barth¹ and Patricia L. Conklin²

¹Boyce Thompson Institute for Plant Research, Tower Road, Ithaca, NY 14853, USA, and

²Department of Biological Sciences, 223 Bowers Hall, State University of New York College at Cortland, Cortland, NY 13045, USA

Received 8 December 2002; revised 6 April 2003; accepted 14 April 2003.

*For correspondence (fax +1 607 753 2927; e-mail conklinp@cortland.edu).

Summary

Under optimal growth conditions (120 $\mu\text{mol photons m}^{-2} \text{sec}^{-1}$ photosynthetically active radiation (PAR), 16-h photoperiod), the recessive ozone-sensitive *Arabidopsis thaliana* L. Heynh. mutant *lcd1-1* exhibits a pale phenotype compared to the wild type. Confocal and multiphoton microscopy revealed that the paleness of *lcd1-1* is because of a lower cell density in the leaf palisade parenchyma, resulting in decreased chlorophyll content. When exposed to ozone, *lcd1-1* leaves become paler and contain an increased amount of the lipid peroxidation product malondialdehyde compared to the wild type, suggesting that *lcd1-1* suffers from elevated levels of reactive oxygen species (ROS) generated in the apoplast. Infection of leaves with virulent *Pseudomonas syringae* reveals higher bacterial growth as well as lower pathogenesis-related protein 1 (PR-1) and PR-5 expression in *lcd1-1* than in the wild type. When the wild type and *lcd1-1* are exposed to short-term high-light stress, leaves do not bleach in *lcd1-1* and potential activities of photosystems I (PSI) and II (PSII) decrease to a similar extent in both the genotypes, indicating that the photosynthetic apparatus is not affected by *lcd1-1* mutation. The *LCD1* gene, found to contain a nonsense mutation in the mutant, has been identified. It is located at the bottom of chromosome 2 of the *Arabidopsis* genome. However, the function of the protein encoded by *LCD1* is not yet known. We hypothesize that *LCD1* plays a role in normal leaf development, and that the increased sensitivity to ozone and virulent *P. syringae* is a secondary effect that presumably results from the lower-cell-density phenotype in *lcd1-1*.

Keywords: ozone, reactive oxygen species, microscopy, positional cloning, virulent pathogen, photoinhibition.

Introduction

Plants are routinely subjected to changes in their environment. Adverse environmental conditions that can negatively affect plant growth and development are believed to result partially from enhanced generation of reactive oxygen species (ROS) such as superoxide anion radicals, singlet oxygen, hydrogen peroxide, and hydroxyl radicals (oxidative stress). ROS are formed in various locations, both in stressed and unstressed leaves (Halliwell and Gutteridge, 1989). ROS are very deleterious as they can oxidize biomolecules, such as pigments, proteins, lipids, and nucleic acids (Padh, 1990). Plants have evolved a complex system of enzymatic and non-enzymatic antioxidant mechanisms to de-toxify harmful oxygen species and, thus, to prevent oxidation of cellular components (Asada, 1994; for a review, see Grene, 2002).

The air pollutant ozone has become a widely used tool to study cell responses induced by ROS. Ozone is very toxic to biological organisms, because it spontaneously dismutates or reacts with cellular components, generating ROS (reviewed by Rao *et al.*, 2000). Ozone has been shown to initiate cell-death processes that are referred to as programmed cell death (PCD) in animals. In plants, PCD is exemplified by the hypersensitive response upon pathogen attack (Levine *et al.*, 1994; Tenhaken *et al.*, 1995). The unique ability of ozone to mimic several pathogen-induced responses greatly aids in studying signaling pathways that cumulate in PCD, resistance and/or the induction of defense genes. Pathogenesis-related proteins (PRs) are useful markers to assess plant defense responses against pathogen attack (Van Loon, 1997).

The formation of ROS is a consequence of metabolic processes such as photosynthesis and respiration. In unstressed plants, generation and de-toxification of ROS are balanced. However, when plants encounter unfavorable environmental conditions, the production of ROS may exceed the capacity of ROS-scavenging systems. For example, absorption of light energy that is in excess of photosynthetic energy utilization leads to the formation of ROS, resulting in a decrease in photosynthetic activity. This has been defined as photoinhibition, which is comprised of both damaging and regulatory protective processes (Aro *et al.*, 1993; Krause, 1988). Photoinhibition can be induced in a variety of plant species (Long *et al.*, 1994). A number of adverse environmental conditions can cause photoinhibition, e.g. chilling temperatures when rates of carbon metabolism are reduced (Huner *et al.*, 1995; Krause, 1994), excessive light (Krause *et al.*, 1995; Powles, 1984; Thiele *et al.*, 1997), UV radiation (Krause *et al.*, 1999), heat or drought. Both photosystem I (PSI) and photosystem II (PSII) have been shown to be affected under photoinhibitory conditions. In both cases, ROS are involved in the inactivation process (Barth *et al.*, 2001; Sonoike, 1996; Tjus *et al.*, 2001). Plants possess a number of mechanisms to protect the photosynthetic apparatus from photo-oxidative damage. Carotenoids and the xanthophyll cycle play important roles in the dissipation of excess excitation energy to avoid the generation of ROS (Codgell and Frank, 1987; Demmig-Adams, 1990; Eskling *et al.*, 1997). The xanthophyll cycle has also been implicated to provide protection against lipid peroxidation (Havaux *et al.*, 2000). In addition, plants possess a complex antioxidative scavenging system in the chloroplast that is linked to the ascorbate–glutathione cycle (Asada, 1999; Grene, 2002).

Mutant plants that are deficient in protective mechanisms are useful tools to better understand this complex defense system that plants utilize to protect themselves against oxidative stress.

In this study, our goal is to better understand the molecular, biochemical, and physiological basis of the *Arabidopsis thaliana lcd1-1* (*lcd*: lower cell density, formerly named *soz2*: sensitive to ozone) mutant phenotype. The *lcd1-1* mutant was isolated by virtue of its sensitivity to the air-pollutant ozone together with the ozone-sensitive *vtc1* mutant (originally named *soz1*), which has been shown to be deficient in an L-ascorbic acid biosynthetic enzyme (Conklin *et al.*, 1996, 1999). In contrast to *vtc1*, *lcd1-1* shows a characteristic pale phenotype compared to the wild type when grown at 120 $\mu\text{mol photons m}^{-2} \text{sec}^{-1}$ photosynthetically active radiation (PAR). Also, *lcd1-1* is deficient neither in L-ascorbic acid nor in glutathione. In order to characterize the *lcd1-1* mutant, a multidisciplinary approach was used. The morphology of *lcd1-1* was analyzed *in vivo* by confocal and multiphoton microscopy. To elucidate whether *lcd1-1* has a defect in a protective mechanism against oxidative

stress, as is implicated by its sensitivity to ozone, we studied physiological responses of the mutant compared to the wild type, when both the genotypes were subjected to several ROS-generating conditions. Finally, the genetic defect in *lcd1-1* was identified with the use of a combined positional cloning and transgenic complementation approach.

Results

Isolation and initial characterization of lcd1-1

The intrinsic tolerance of the wild-type *A. thaliana* L. Heynh. (ecotype Columbia) to ozone facilitates the isolation of ozone-sensitive mutants (Conklin *et al.*, 1996). The *A. thaliana* mutant *lcd1-1* that was generated by ethyl methane-sulfonate (EMS) mutagenesis of Columbia wild-type seed (Barczak *et al.*, 1995) was isolated in the same mutant screen as was *vtc1* (previously named *soz1*; Conklin *et al.*, 1996). The *lcd1-1* mutant was one of the three mutants that exhibited inheritable ozone sensitivity in this ozone screen.

Compared to non-fumigated plants (Figure 1a,b), exposure to ozone (250–300 nl l^{-1}) did not result in visible damage in the wild type (Figure 1c), whereas *lcd1-1* leaves became paler and had a bleached appearance (Figure 1d). Analysis of ozone-treated and cell-wall stained leaves by multiphoton microscopy revealed that cells of the wild type were undamaged (Figure 1e,g), whereas cells in *lcd1-1* collapsed, resulting in complete disintegration of the leaf tissue after ozone exposure (Figure 1f,h).

Determination of the lipid peroxidation product malondialdehyde (MDA) revealed a twofold increase in the content of MDA per gram DW in the mutant compared to the wild type after 4 h of ozone fumigation (400 nl l^{-1} ; data not shown), indicating that ozone-treated *lcd1-1* may suffer from increased levels of ROS. Further biochemical analyses have shown that in comparison to the wild type, *lcd1-1* is deficient neither in L-ascorbic acid nor in glutathione. Although *lcd1-1* is sensitive to the ROS-generating pollutant ozone, it does not appear to be paraquat-sensitive (data not shown).

Leaf palisade parenchyma density decreased in lcd1-1

When grown at 120 $\mu\text{mol photons m}^{-2} \text{sec}^{-1}$ PAR, the *lcd1-1* mutant exhibited a pale interveinal phenotype compared to the wild type (Figure 2a,b, insets). This phenotype was further characterized at high resolution by confocal and multiphoton laser scanning microscopy by analyzing at least two regions of three to five independent leaves of each genotype.

Figure 2(a,b) shows three-dimensional confocal image re-constructions of 2-week-old leaves of the wild type

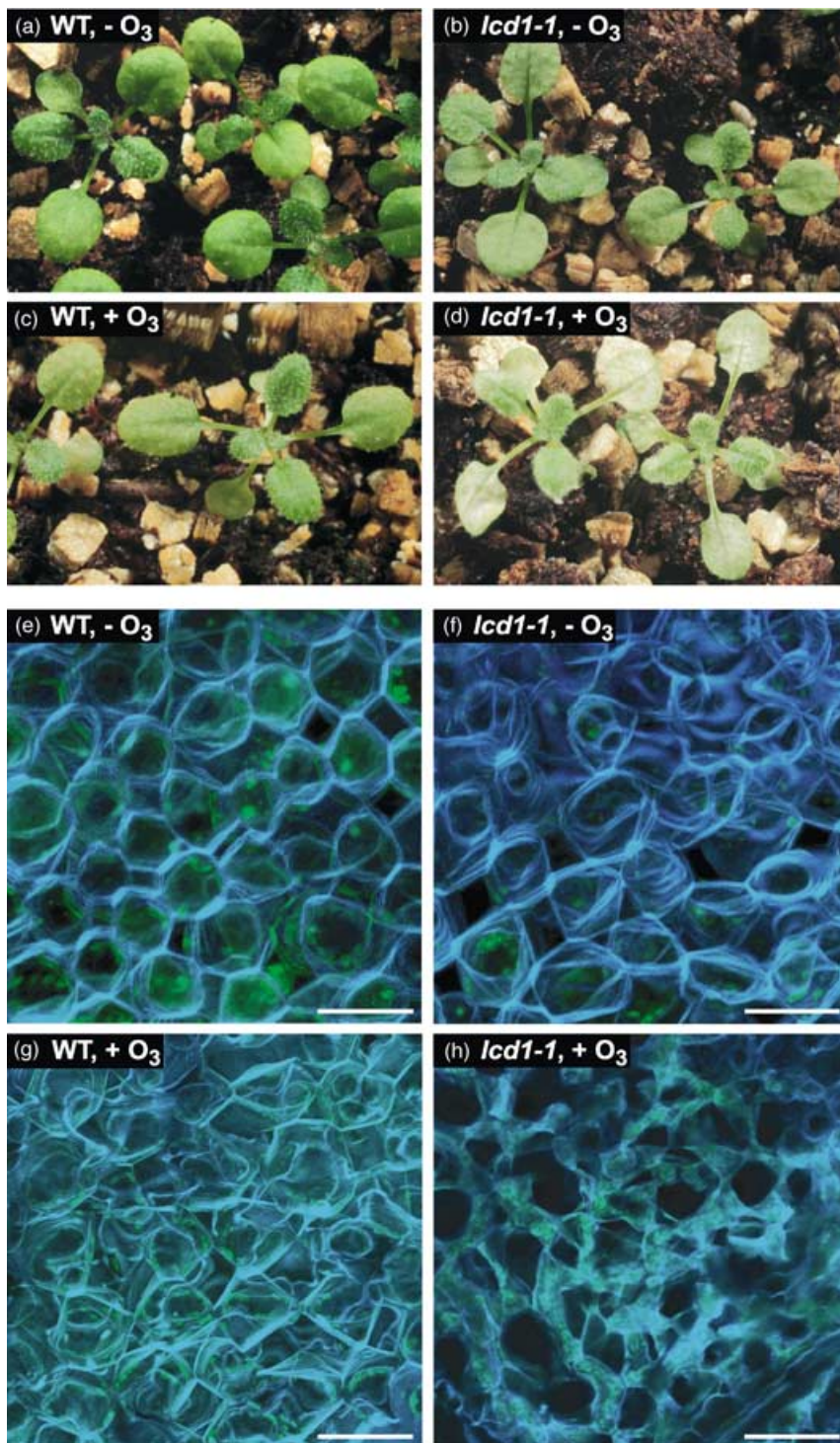


Figure 1. Phenotypes of non-ozone and ozone-treated wild-type and *lcd1-1* plants.

(a,b) Phenotypes of the wild-type and *lcd1-1* plants when 2 weeks old and grown at $120 \mu\text{mol photons m}^{-2} \text{sec}^{-1}$ photosynthetically active radiation (PAR), 16-h photoperiod.

(c,d) Two-week-old wild-type and *lcd1-1* plants were fumigated with ozone for 8 h. Photographs were taken 16 h after ozone exposure.

(e,f) Three-dimensional multiphoton images of 2-week-old wild-type and *lcd1-1* plants grown as in (a) and (b) and infiltrated with 0.1% calcofluor white to visualize the cell wall.

(g,h) Three-dimensional multiphoton images of 2-week-old wild-type and *lcd1-1* plants exposed to ozone for 8 h and cell wall stained with calcofluor white. Images were taken 16 h after ozone treatment. Ozone concentration was $250\text{--}300 \text{ nl l}^{-1}$ in all cases. Scale bars: $50 \mu\text{m}$ (e–h). All experiments and microscopy analyses were repeated independently at least four times.

and *lcd1-1* plants. It is immediately obvious that *lcd1-1* leaves contain fewer cells per unit area than the wild type. As seen in Figure 2(a,b), the wild type and *lcd1-1* did not appear to differ in the number of chloroplasts per cell or in overall cell size. Moreover, the wild type and *lcd1-1* exhibited the same amount of chlorophyll fluorescence, suggest-

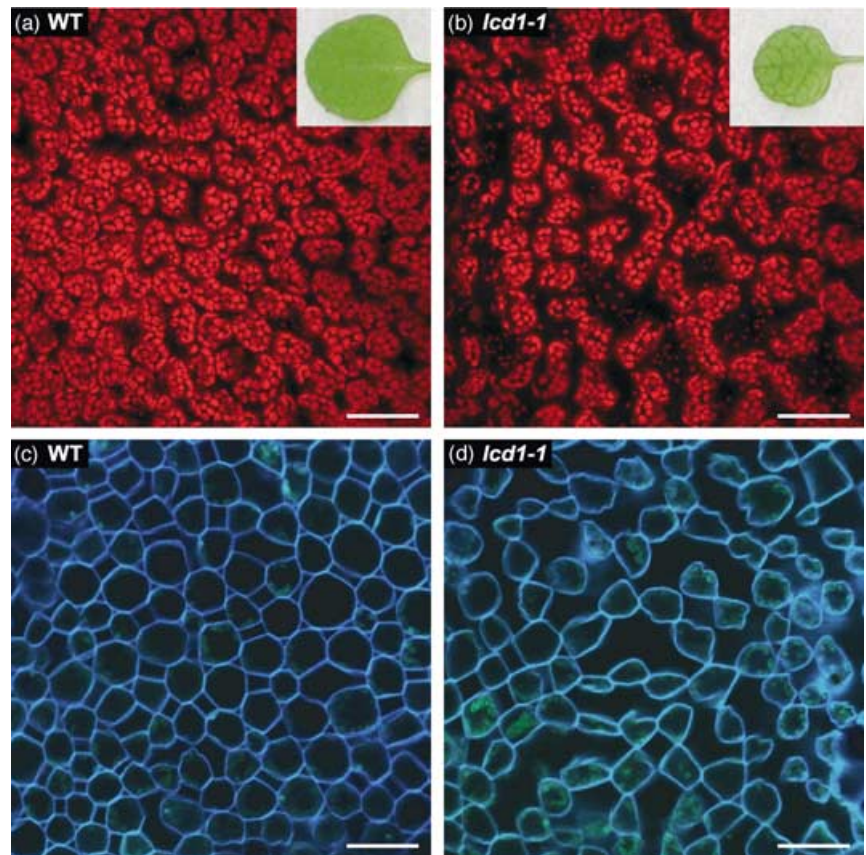
ing that the genotypes do not differ in the amount of chlorophyll per chloroplast and per cell, respectively.

In order to clarify whether the lower cell density in *lcd1-1* is because of a larger interstitial space between the cells or is a consequence of thicker cell walls in *lcd1-1*, multiphoton microscopy was employed. To visualize the cell wall, leaves

Figure 2. Confocal and multiphoton microscopy of 2-week-old wild-type and *lcd1-1* plants. (a,b) Three-dimensional confocal microscopy image re-constructions of the wild-type and *lcd1-1* plants. Insets in (a) and (b): leaves of 2-week-old wild-type and *lcd1-1* mutant plants, respectively, to visualize the interveinal paleness of *lcd1-1*.

(c,d) Multiphoton microscopy images of the wild type and *lcd1-1*. To specifically stain the cell wall, leaves were infiltrated with 0.1% calcofluor white using a syringe without a needle. Images were taken from the middle upper (adaxial) side of the leaf. At least two regions of three to five independent leaves of each genotype were investigated from the tip to the base of the leaf. In all cases, plants were grown as described in Figure 1.

Scale bars: 100 μ m (a–d).



of 2-week-old wild-type and *lcd1-1* plants were infiltrated with 0.1% calcofluor white. As shown in Figure 2(c,d), the wild-type and *lcd1-1* plants did not differ in the thickness of their cell walls, but rather in the amount of the interstitial space between cells. This space is much larger in *lcd1-1*. Detailed analyses of the wild-type and *lcd1-1* leaves revealed that the lower cell density in the mutant is restricted to the palisade parenchyma, and occurs from the base to the tip of the leaf. The vascular elements as well as the epidermis appear normal. The cell density of tissues composing the roots, floral organs, and seeds is not affected by *lcd1-1* mutation (data not shown). These results suggest that the *LCD1* gene is most likely expressed in leaves or the leaf meristem, and that the *LCD1* gene product is required for normal post-embryonic leaf development.

The reduced parenchyma cell density in lcd1-1 results in a lower chlorophyll content and a decreased biomass production per leaf area

As mentioned previously, and as seen in Figure 1(b) and the inset of Figure 2(b), *lcd1-1* plants appear pale to the eye, most likely as a result of a lower chlorophyll content of the leaf resulting from the lower cell density. Indeed, total chlorophyll content (Chl *a* + *b*) per leaf area is significantly diminished in *lcd1-1* (Table 1). However, when chlorophyll

content was based on FW or DW, no significant differences were obtained between the wild type and mutant, as expected (data not shown). Based on leaf area, other chloroplast pigments, such as neoxanthin, lutein, β -carotin, and the xanthophyll cycle pigments violaxanthin, antheraxanthin, and zeaxanthin were also lower in the mutant compared to the wild type as a result of the lower cell density in *lcd1-1* (data not shown). However, when based on total chlorophyll, FW, or DW, no significant differences in other chloroplast pigments were observed between the wild type and *lcd1-1* (data not shown), indicating that the *lcd1-1* mutation did not cause changes in the pigment composition of the photosynthetic apparatus per cell.

Figure 3 shows light-saturation curves for CO₂ assimilation, which was measured in leaves of four individual plants of each genotype. The rate of photosynthesis based on leaf area is slightly lower in *lcd1-1* than in the wild type (Figure 3a). However, when CO₂ uptake was based on FW (data not shown) or DW (Figure 3b), no differences were observed between both the genotypes. Finally, the wild type and *lcd1-1* did not differ significantly in the stomatal ratios (data not shown).

The lower photosynthesis rate in *lcd1-1* predicts a lower biomass production in the mutant. As shown in Figure 1(b) and the inset of Figures 2(b) and 6(c), growth of *lcd1-1* is somewhat retarded. Compared to the wild type, FW and

Table 1 Total chlorophyll content and biomass per area are reduced in the *lcd1-1* mutant

Genotype	Chl <i>a</i> + <i>b</i> ($\mu\text{mol m}^{-2}$)	FW (mg cm^{-2})	DW (mg cm^{-2})	DW:FW (%)
WT	248 \pm 23	23.93 \pm 2.65	2.27 \pm 0.19	9.53 \pm 0.97
<i>lcd1-1</i>	181 \pm 18*	19.51 \pm 1.35*	1.78 \pm 0.21*	9.14 \pm 0.86

Total chlorophyll (Chl *a* + *b*) content as well as FW and DW were determined in 5-week-old wild-type and *lcd1-1* plants grown at 120 $\mu\text{mol photons m}^{-2} \text{sec}^{-1}$ photosynthetically active radiation (PAR). Values represent means \pm SD of five individual plants of each genotype. Mature leaves were taken from the middle of the rosette. Asterisks indicate significant differences between the wild type and mutant.

DW were significantly lower by about 20% in *lcd1-1*, whereas both genotypes did not differ in their DW:FW ratio (Table 1). Therefore, reduction in biomass in the mutant is most likely a result of the overall reduced number of cells per leaf area, rather than diminished biomass production per cell.

lcd1-1 does not have increased sensitivity to high-light stress

To assess the sensitivity of *lcd1-1* to high-light stress, leaves of three individual wild-type and *lcd1-1* plants were exposed to 2000 $\mu\text{mol photons m}^{-2} \text{sec}^{-1}$ PAR at both 20 and 8°C, and potential activities of PSI and PSII were deter-

mined. After 90 min high light at 20°C, PSI activity was diminished by only 20–25% of control in both the genotypes (Figure 4a), whereas potential PSII efficiency decreased to about 60% of control in the wild type and *lcd1-1* (Figure 4b). When exposed to high light at 8°C, i.e. under more severe ROS-generating conditions, again no differences in the potential activities of PSI and PSII were observed between both the genotypes (data not shown). It is also noteworthy that at both temperatures, the wild type and *lcd1-1* did not

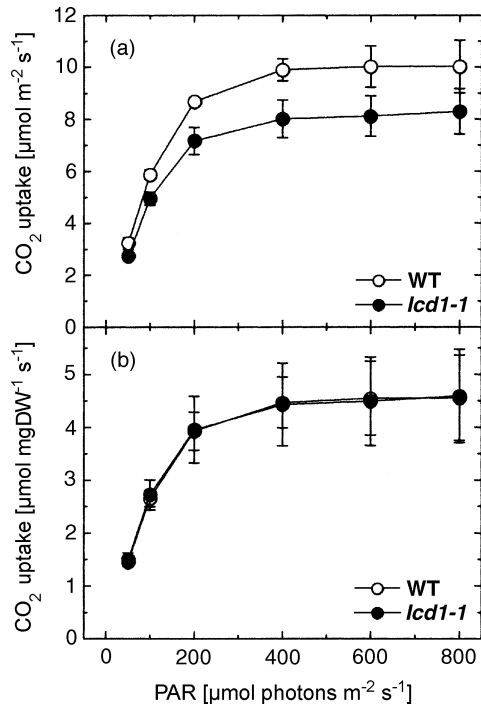


Figure 3. Light saturation curves for CO₂ uptake of 5-week-old wild-type and *lcd1-1* plants.

Gas-exchange measurements were performed at atmospheric CO₂ concentrations.

(a) CO₂ assimilation rate based on leaf area.

(b) CO₂ assimilation rate based on DW. Means \pm SD of four leaves from different plants of each genotype are given. SD is not shown where smaller than symbols.

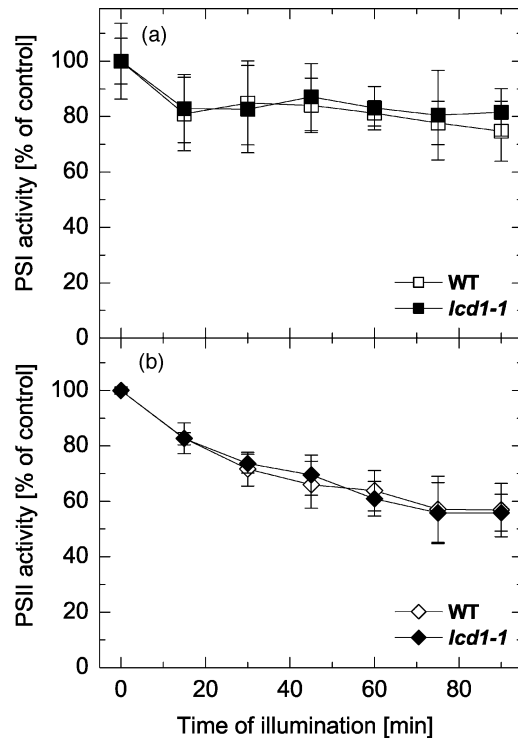


Figure 4. Effects of short-term high-light exposure on the wild-type and *lcd1-1* plants.

Leaf discs of 5-week-old wild-type and *lcd1-1* plants were illuminated with 2000 $\mu\text{mol photons m}^{-2} \text{sec}^{-1}$ photosynthetically active radiation (PAR) at 20°C.

(a) Potential activity of PSI determined as P700 absorbance change at 810 nm (ΔA_{max}). ΔA_{max} of controls (relative units): 13.5 \pm 1.1 (wild type), 11.5 \pm 1.6 (*lcd1-1*).

(b) Potential efficiency of PSII measured as ratio of variable to maximum chlorophyll *a* fluorescence (F_v/F_m). F_v/F_m ratios of controls: 0.795 \pm 0.024 (wild type), 0.800 \pm 0.013 (*lcd1-1*). Means \pm SD of nine (PSII) or means of six (PSI) independent experiments are given. SD is not shown where smaller than symbols.

differ in their xanthophyll cycle activity, i.e. in the de-epoxidation kinetics of violaxanthin to antheraxanthin and zeaxanthin (data not shown).

Responses to biotic stress – lcd1-1 is more susceptible to a virulent pathogen

Inoculation of the wild-type and *lcd1-1* mutant plants with *Pseudomonas syringae* pv. *maculicola* ES4326 (10^6 Colony-Forming Units (CFU) ml^{-1}) results in lesions with a spreading chlorosis that appears 48 h post-inoculation. These lesions, which were observed in two other experiments, are significantly larger in *lcd1-1* than in the wild type (Figure 5a), indicating that the mutant is more susceptible to ES4326. This is confirmed by the growth of the bacterium in infected leaves. ES4326 multiplies at a higher rate in *lcd1-1* than in the wild type (Figure 5b). Although not significant at all time-points, 2–3 days post-inoculation, the bacterial titer was significantly higher in infected leaves of the mutant than in those of the wild type. The same trend was seen in four additional independent experiments. Western blot analysis revealed that inoculation with ES4326 elicits, as expected, the accumulation of PR-1 and PR-5 in both the genotypes. However, independent analyses have shown that the accumulation of PR-1 (N = 2, not shown) and PR-5 protein (N = 3) was significantly lower in *lcd1-1* than in the wild type (Figure 5c).

Identification of the LCD1 gene

Segregation analysis revealed that the ozone-sensitive phenotype of *lcd1-1* is conferred by a single monogenic recessive allele (data not shown). The pale phenotype of *lcd1-1* co-segregates with ozone-sensitivity. An F_2 of a back-cross between the ozone-resistant progenitor (Col-0 ecotype) and *lcd1-1* was fumigated with ozone (approximately 300 nl l^{-1}). Only plants with the characteristic interveinal paleness of *lcd1-1* exhibited visible damage by ozone, whereas phenotypically the wild-type plants did not. Co-segregation of the pale phenotype and ozone-sensitivity in the back-cross line occurred in a 3 : 1 ratio (data not shown). For positional cloning of the *lcd1-1* mutation, an F_2 -mapping population was developed from a cross between *lcd1-1* (Col-0 background) and *Ler*. Using a small number of mapping lines (which were identified by the pale phenotype observed under ambient conditions), the *LCD1* locus was initially mapped to chromosome 2 of the *A. thaliana* genome, approximately 0.7 cM centromere proximal from the simple sequence-length polymorphism marker (SSLP) nga168 and approximately 4.3 cM from the previously identified *VTC1* gene (Figure 6a; Conklin *et al.*, 1999).

Using 2090 individuals from the original mapping population (Figure 6b), the *LCD1* locus was narrowed genetically to a 19-kb region on BAC T8P21, a BAC containing the

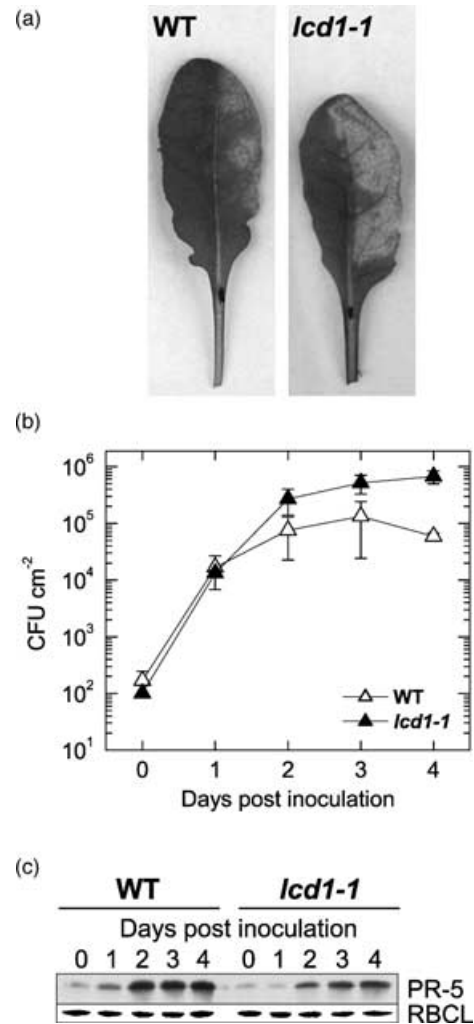


Figure 5. Responses of the wild type and *lcd1-1* upon infection with virulent *Pseudomonas syringae* pv. *maculicola* ES4326. Plants in this experiment were 5 weeks old.

(a) Disease symptoms of the wild-type and *lcd1-1* plants infiltrated with ES4326. The middle of the lower side of leaves was infiltrated with a bacterial suspension at 10^5 Colony-Forming Units (CFU) ml^{-1} . Photographs were taken 72 h after inoculation. This experiment was repeated two times with similar results on four to five leaves of the wild-type and *lcd1-1* mutant plants per experiment.

(b) Growth curve of ES4326 in the wild-type and *lcd1-1* plants. Plants were inoculated with a bacterial suspension containing 10^5 CFU ml^{-1} . At the indicated times, bacterial growth in leaves (as CFU cm^{-2} of leaf area) was determined as described in Experimental procedures. Mean values \pm SD of three to four individual plants of a representative experiment are shown. SD is not shown where smaller than symbols. The same trend was seen in four additional independent experiments in which four plants of each genotype per experiment were inoculated.

(c) Western blot analysis of the wild-type and *lcd1-1* leaves infiltrated with ES4326 at 10^5 CFU ml^{-1} to show induction of PR-1 (not shown) and PR-5 proteins. The large subunit of RUBISCO (RBCL) was visualized by Ponceau Red staining and served as a control for equal loading. Induction of PR-1 and PR-5 was tested in three independent inoculation experiments with similar results.

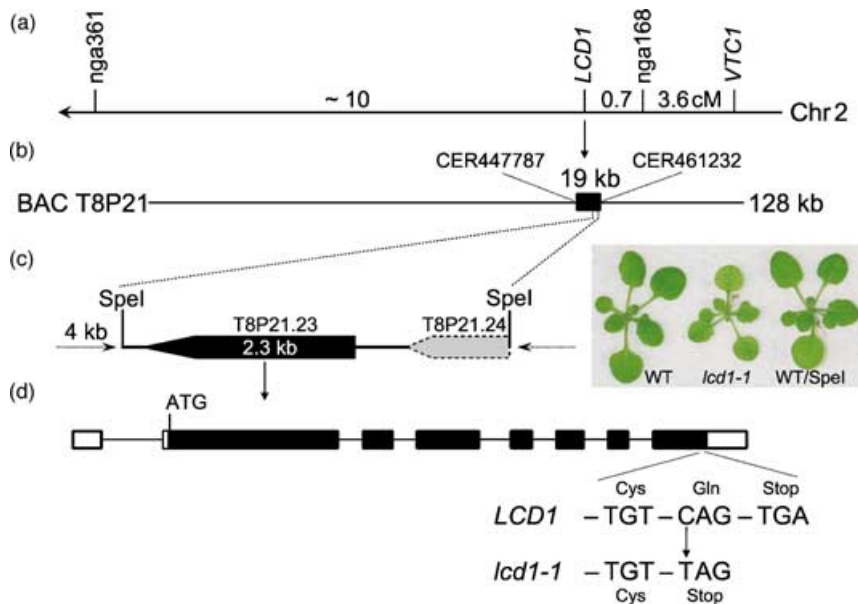


Figure 6. Identification of *LCD1* gene.

(a) Genetic and physical characterization of the *LCD1* locus.

(b) The *LCD1* locus within a 19-kb region of BAC T8P21 was narrowed down by a positional cloning approach. Shown are the Cereon ID numbers that identify the polymorphisms that have been used to genetically narrow the *LCD1* locus to the 19-kb region (see Experimental procedures for details).

(c) A 4-kb *SpeI* fragment from BAC T8P21 that complemented the *lcd1-1* mutation when present as a transgene in *lcd1-1* mutant plants. Photographs of the wild-type, *lcd1-1*, and a transgenic complementation line are shown.

(d) Structure of the *LCD1* transcribed region and nonsense mutation in *lcd1-1*. Unshaded rectangles, non-coding sequences present in the *LCD1* cDNA; black rectangles, exons encoding *LCD1*; thin lines, location of intron sequences.

128 kb of chromosome 2 located between 69.5 and 70.5 cM on the Lister and Dean RI map (<http://arabidopsis.org>). For this marker-driven mapping, InDel markers (small nucleotide insertions or deletions in Col-0 or Ler) and single nucleotide polymorphisms (SNPs) from the Monsanto Arabidopsis Polymorphism Collection (<http://www.arabidopsis.org/Cereon/index.html>) in this region were utilized. Specifically, the *LCD1* gene was located within this 19-kb region upon the discovery of recombination breakpoints in one F₂-mapping line between the centromeric proximal marker CER447787 and *LCD1* and in a single F₂-mapping line between *LCD1*, and the centromeric distal marker CER461232. This 19-kb region contains nine candidate genes (Figure 6b).

To identify which of these nine genes encodes *LCD1*, a transgenic complementation approach was utilized. The T8P21 BAC-DNA was restriction-digested into fragments that contained two or three genes of the 19-kb *LCD1* region. These fragments were used in *Agrobacterium*-mediated transformations of *lcd1-1* individuals. One of these fragments (a 5.4-kb *EcoRV* fragment) contains the open-reading frames (ORFs) T8P21.22 (predicted to encode a protein of the lipid transfer protein family) and T8P21.23 (predicted to encode an expressed protein with unknown function) in full length and the 3'-half of T8P21.24. Transformants containing this 5.4-kb fragment (identified by their resistance to the herbicide BASTA) exhibit a wild-type phenotype (data not shown), indicating that the *lcd1-1* mutation is complemented by either T8P21.22 or T8P21.23. Transformation of *lcd1-1* mutant plants with a T8P21-BAC-derived restriction fragment, containing only the wild-type transgene of T8P21.23, resulted in transgenic line, exhibiting a wild-type phenotype (Figure 6c), demonstrating that the ORF T8P21.23 is the *LCD1* gene. To further support that the

correct gene was identified, *lcd1-1* lines transformed with a genomic copy of the *LCD1* locus (i.e. transgenic lines containing either the 5.4-kb *EcoRV* or the 4-kb *SpeI* fragment) were exposed to ozone and (in a separate experiment) infected with virulent *P. syringae* ES4326 to verify that the *lcd1-1* phenotypes of ozone and pathogen-sensitivity are complemented as well. All tested *lcd1-1* transgenic complementation lines and the wild-type control were resistant to ozone. Furthermore, these transgenic lines had similar or slightly less susceptibility to pathogen infection than the wild type (data not shown). Finally, sequence analysis was performed to identify the expected point mutation. In ORF T8P21.23, at amino acid 431 relative to the first base in the predicted coding region, cytosine (C) in the wild type is mutated to thymine (T) in the *lcd1-1* mutant. This change is a nonsense mutation that is predicted to convert the final annotated amino acid glutamine in the wild type to a stop codon in the mutant (Figure 6d).

Expression analysis of the *LCD1* gene by competitive RT-PCR (Gilliland *et al.*, 1990) did not reveal significant differences in the amount of a cDNA fragment in the *LCD1* gene specifically amplified from total RNA isolated from the wild type and *lcd1-1*. The amount of the wild-type *LCD1* cDNA was estimated to be 6.5 ± 1.3 ($n = 4$) and that of *lcd1-1* 10 ± 2.6 ($n = 3$) from 1 μ g total RNA starting material.

LCD1 encodes an unknown protein

The sequence of BAC T8P21 was annotated by TAIR and TIGR. ORF T8P21.23 was identified as an expressed protein of unknown function (http://www.tigr.org/tigr-scripts/euk_manatee/shared/ORF_infopage.cgi?db=ath1&orf=44466.t00016). The sequence of a full-length cDNA using primers in the 5'-UTR and 3'-UTR was obtained to define all introns

A. thaliana	NP_181322	(432)	LPSSVFEAERPGCRFSAOQRJATYFYKGYMYGVGFGCGLVGGOGIANLIMTAKRNINK--	351
A. thaliana	NP_197671	(433)	LPSSVFEAERPGCKRFSVNRJATFFYKGLLYGVSFGGCGLVGGOGIANLIMTAKRSVKKR--	352
E. esula	AAF31706	(268)	LPSSVFEAERPGCRFSILKORVATYFYKGVLYGVSFGGCGLVGGOGIANLIMTAKRSIKK--	187
A. thaliana	NP_568280	(386)	CPDNLKQVALSCTSYTLLQRIGAITRNGAKLFAVGTSSLVGTATINAFITKARKAVDQN-	302
A. thaliana	NP_187476	(337)	CPSSHMFEGQS---STVMNRFGLVYKGMVFASVGLAAGLVGTALSNGLIMLRKKMDPS-	245
O. sativa	BAB68096	(723)	LPDNLKQKGMCSQSWNTNORFASVLMCSIKLAGVGEISSICAGVASDVLVYARVLRPST	599
A. thaliana	NP_181322	(432)	--SEENIEVPPLIKSAALWGVFLSVSSNTRYQIINGLERVVEASFFAKKF--PAAAMAFTV	408
A. thaliana	NP_197671	(433)	--SEEDVPIPPLEBSAALWGVFLGLSSNARYQIINGLERVVEGSSATAKRI--PVMAMAFTV	409
E. esula	AAF31706	(268)	--SEEDIEVPPLVCSAVLWGVFLAVSSNTRYQIINGLESLEKSPAKKVV--PVMAMAFTV	244
A. thaliana	NP_568280	(386)	--SEGEVETVPIVSTSVAYGVYMAVSSNLRYOIVAGVIEQRLLLEMLHQH--KVALSALCF	359
A. thaliana	NP_187476	(337)	--FETPNKPEPTVLNLSLTWATHMGVSNARYQITLNGIEFLAK--VLP----PLVFKTSVI	298
O. sativa	BAB68096	(723)	SVETARRRTPHWKSATVYSCFLGTSANLRYOIVAGLVEHRLGEYLMAYYNOPELQANLLSF	659
A. thaliana	NP_181322	(432)	GVRLANNHYGGMOFVDWARLSGCG-----	432
A. thaliana	NP_197671	(433)	GVRFANNHYGGMOFVDWARLSGVQ-----	433
E. esula	AAF31706	(268)	GVRFANNHYGGMOFVDWARLSGVQ-----	268
A. thaliana	NP_568280	(386)	AVRTCTNFLGLSLLDVYARLIGTKSH-----	386
A. thaliana	NP_187476	(337)	VLRCANNVAGGSEVLLARMTGSSVEEKTEISEKEKDD-----	337
O. sativa	BAB68096	(723)	VSRTINSYWGTCWILLARATGLCTSKKELPSPEISNLPDMPLECGTTEVQNMDSSNKQ	719

Figure 7. Comparison of the C-terminus of the *Arabidopsis* ORF T8P21.23 with homologous regions of other predicted plant proteins. Numbers next to the species names and number in brackets represent the GenBank accession numbers and the predicted number of amino acids that encode the protein, respectively. Highlighted in bold is the protein encoded by ORF T8P21.23 (LCD1). The arrow indicates the last wild-type amino acid glutamine (Q) that is converted to a stop codon in *lcd1-1*.

and exons, verifying the annotation neither by TAIR nor by TIGR. Both databases have annotated ORF T8P21.23 as a gene comprising of five exons encoding a protein consisting of 348 amino acids. According to our sequencing results, *LCD1* contains seven exons (cf. Figure 6d). The stop codon for the *LCD1* gene was annotated by TAIR as TAA in exon 5 (position 15806814), which is followed by a UTR of 155 bp (<http://www.arabidopsis.org/servlets/sv?action=seq&start=15804697&length=10000&band=0&option2=0>). However, our sequence data of a cDNA amplified from both Col-0 wild-type and *lcd1-1* total RNA demonstrate that this stop codon is in an intron starting at position 15806813 and that the intron is 94 bp in length. It should be noted that the genomic sequence of the *LCD1* locus is consistent with the database annotation, except that the 3'-UTR is longer by nine nucleotides. Our sequencing results confirm the annotated full-length cDNA clones OBO239 (GenBank accession no. F19753) and OBO254 (GenBank accession no. F19749), with only minor differences in the 5'- and 3'-UTR and a base-pair change at position 1197 from the start codon. Therefore, *LCD1* must encode a protein of 432 amino acids.

This is consistent with the annotation by the Munich Information Center for Protein Sequences (MIPS; http://mips.gsf.de/cgi-bin/proj/thal/search_gene?code=At2g37860). The predicted approximately 47-kDa LCD1 was annotated as a putative transmembrane protein of 432 amino acids. This predicted protein has amino acid similarity with other unknown predicted proteins in *A. thaliana* and other plant species (Figure 7; <http://www.ncbi.nlm.nih.gov/blast/Blast.cgi>). One protein in the *Arabidopsis* genome located on chromosome 5 (accession no. NP_197671), and an unknown protein in *Euphorbia esula* (accession no. AAF31706) are 72 and 73%, respectively, identical to LCD1. The C-terminal portions of the last three

Arabidopsis and *Oryza* proteins listed in Figure 7 show only 26–30% identity with LCD1. However, note that the glutamine, the final amino acid in LCD1, is highly conserved in the LCD1 protein homologs. It is this amino acid that is converted to a stop codon by a nonsense mutation in the mutant *lcd1-1*.

Discussion

The novel ozone-sensitive *A. thaliana* mutant *lcd1-1* has been characterized by using a multidisciplinary approach that combines genetic, physiological, and microscopy analyses.

The *lcd1-1* mutant was isolated as a result of its sensitivity to the air pollutant ozone (cf. Figure 1). Ozone reacts with plant cell wall phenolics, olefinic compounds, and unsaturated lipids, rapidly generating ROS in the apoplast (reviewed by Mudd, 1997). The fact that leaves of *lcd1-1* bleach upon ozone exposure suggests that the mutant may have a defect in a protective mechanism against ROS.

Confocal and multiphoton microscopy greatly aided in the morphologic characterization of the *lcd1-1* mutant *in vivo*. The pale phenotype of this mutant, when grown under standard *Arabidopsis* growth conditions with a 16-h photoperiod, is a result of a specific reduction in leaf palisade parenchyma cells (cf. Figure 2). The epidermis and vascular elements appear normal. This suggests that *lcd1-1* may have a defect in cell division of mesophyll cells. *Arabidopsis* mutants with normal cell size but a reduced number of cells per leaf blade have been reported previously. The *curly leaf* (*clf*) mutant grows as wild type, but the foliage leaves are significantly smaller than those of the wild type because cell elongation and the number of cells are reduced in *clf* (Kim *et al.*, 1998). The *compact rosette* (*cro4-1*) mutant has short leaves with leaf blades

of slightly reduced width compared to the wild type. This mutant has cells of normal size but a reduced number in the lamina (Tsukaya, 2002). Unlike these previously described mutants, leaves of *lcd1-1* are only slightly smaller than the wild type, and they do not differ in leaf shape (cf. Figures 1a,b, 2a,b (insets) and 6c), indicating that leaf expansion is not affected in *lcd1-1*.

The pale phenotype of *lcd1-1* was originally thought to be a result of a defect in chlorophyll biosynthesis or in an accessory (light-harvesting) pigment that is also involved in photo-protection, such as xanthophyll cycle pigments or β -carotin. We predicted that the obvious lower chlorophyll content (cf. Table 1) and/or a defect in a protective pigment would affect photosynthetic activity in the mutant. Therefore, we analyzed other chlorophyll pigments, determined potential activities of PSI and PSII under light stress, as well as measured CO₂ assimilation in non-stressed and stressed leaves of the wild-type and *lcd1-1* plants. Surprisingly, no deficiency in other chloroplast pigments was observed on a per cell basis (data not shown). Also, the CO₂ assimilation rates per cell (Figure 3), as well as the potential activities of both PSI and PSII (Figure 4), are the same in the wild type and *lcd1-1*. These data indicate that the photosynthetic apparatus is not affected by the *lcd1-1* mutation, and that there is no defect in a chloroplast-protective mechanism in the mutant. However, growth of *lcd1-1* is slightly retarded. Like the reduction in chlorophyll, this observation can be explained by the decreased number of cells in the mutant (cf. Figures 2 and 3; Table 1).

The fact that *lcd1-1* is more susceptible to ozone implies that the mutant may suffer from enhanced levels of ROS generated in the apoplast. The ozone sensitivity of *lcd1-1* parallels the higher susceptibility of *lcd1-1* to virulent *P. syringae* (cf. Figures 1c,d and 5a,b). Several studies have demonstrated that ozone sensitivity resembles the pathogen response (Overmyer *et al.*, 2000; Rao and Davis, 1999; Schraudner *et al.*, 1998). It has been shown that *P. syringae* multiplies in the apoplast of the host plant. To attain a high population in the intercellular space, *P. syringae* produces appropriate virulence factors to cause the host cells to leak nutrients and water into the apoplast. Simultaneously, the bacteria must suppress *Arabidopsis* defense mechanisms that inhibit bacterial proliferation (reviewed by Katagiri *et al.*, 2002). PRs are part of the arsenal of plant-defense proteins induced upon pathogen attack. As PR-1 and PR-5 proteins were analyzed as a portion of total protein and as the cells contain the majority of this protein, one may assume that on a per cell basis, there is less PR-1 and PR-5 protein in *lcd1-1* compared to the wild type (cf. Figure 5c). Hence, the lower induction of PR-1 and PR-5 proteins may contribute to the higher proliferation rate of virulent *P. syringae* in *lcd1-1* (cf. Figure 5b,c).

In summary, the pale phenotype of *lcd1-1* is the result of a lower chlorophyll content that is a result of the lower cell

density in the leaf palisade parenchyma, and is the result of a defect in chlorophyll or carotenoid biosynthesis. Furthermore, we conclude that the *lcd1-1* mutation does not impair photosynthetic activity per cell, but overall biomass production is diminished in *lcd1-1* as a result of the reduced number of cells per leaf blade. Finally, *lcd1-1* does not suffer from ROS produced in the chloroplast under high-light conditions, indicating that the ROS-scavenging system in the chloroplast is not affected in *lcd1-1*. The mutant appears, however, to be susceptible to oxidative stress generated in the apoplast.

How can these different mutant phenotypes be explained? We have two alternative hypotheses. (i) The LCD1 protein plays a role in normal leaf development, perhaps in the cell division of the mesophyll cells. A defective protein and/or absence of this protein causes the *lcd1-1* mutant phenotype of lower cell density that either directly or indirectly affects other cellular processes. (ii) The LCD1 protein is involved in several functions, and therefore, when mutated, results in additional altered phenotypes besides that of a lower cell density.

Our data clearly indicate that LCD1 is involved in cell proliferation that affects leaf development and that this function may be regulated by light, as mutant plants do not exhibit the pale interveinal phenotype when grown under very low light (data not shown). In support of hypothesis (i) we provide evidence that the lower chlorophyll content and the decreased biomass production are most likely a result of the reduced number of leaf parenchyma cells, and not because of an intrinsic defect in photosynthetic activity. The increased ozone and pathogen sensitivity of *lcd1-1* may be at least partially because of the fact that the apoplast is much more abundant in the mutant than in the wild type. Ozone dissolves in the apoplastic space into ROS. As there are fewer cells in *lcd1-1* than in the wild type, more oxygen radicals can attack a single cell in *lcd1-1*, resulting in pronounced tissue damage compared to the wild type. As a result, the defense mechanisms initiated by the *lcd1-1* cells may not be sufficient, i.e. *lcd1-1* may not mount an adequate defense response. Similarly, the higher susceptibility of *lcd1-1* to the virulent pathogen may be a result of the fact that defense mechanisms evolved by each cell are insufficient to suppress multiplication of the bacteria in the apoplast. Moreover, as suggested in Figure 2(d), the cell-to-cell communication within the palisade parenchyma is likely to be affected in the mutant, suggesting that signal transduction may be strongly impaired in the mutant and may perhaps best explain the ozone/pathogen sensitivity.

In case of the alternate hypothesis (ii), the *lcd1-1* mutant may have a defect in the development of the leaf architecture and a defect in at least a subset of the plant-defense response. Therefore, the wild-type LCD1 gene product may function in both these arenas, suggesting that a defect in

LCD1 may result in a pleiotropic mutant phenotype. However, this is purely speculative.

The results presented in this paper strongly support hypothesis (i), indicating that the sensitivity of *lcd1-1* to ozone and virulent *P. syringae* are secondary effects of the lower cell-density phenotype of *lcd1-1*.

From the *lcd1-1* mutant phenotype, we are unable to make any educated guesses as the identity of the LCD1 gene product is not yet known. Therefore, we undertook a positional cloning approach to identify the LCD1 gene. Using a combination of recombination analysis and transgenic complementation, we have identified the LCD1 gene as being T8P21.23, a gene at the bottom of chromosome 2 that was annotated by MIPS as encoding an expressed protein with unknown function. Curiously, the nonsense mutation in *lcd1-1* eliminates only the final carboxy-terminal amino acid in this predicted protein (cf. Figure 6d). One other predicted protein in the *Arabidopsis* genome (NP_197671 on chromosome 5) and a predicted *E. esula* protein (accession no. AAF31706) share high amino acid similarity with LCD1 (cf. Figure 7). Like LCD1, these predicted proteins also have, as yet, unknown functions. It is interesting to note that the last amino acid, glutamine, that is lost in *lcd1-1*, is conserved in these other LCD1 homologs (cf. Figure 7). To our knowledge, no allele of a plant gene has been described thus far that lacks the final amino acid of the C-terminus, resulting in a mutant phenotype. In animal systems, removing the last or the last two amino acids from the C-terminus have been shown to result in complete loss or insufficient activity of the protein (Gary and Bretscher, 1995; Xie *et al.*, 2000).

The MIPS predicts that LCD1 is most likely a transmembrane protein with a prokaryotic membrane lipoprotein lipid attachment site that is targeted to the chloroplast (http://mips.gsf.de/cgi-bin/proj/thal/search_gene?code=At2g37860). Expression analysis of the LCD1 gene was performed by competitive RT-PCR. As the yield and efficiency of the RT reaction is not reflected in this method, and heterogeneity in mRNA may affect the amplified PCR fragments, the absolute quantity of LCD1 mRNA present in the wild type and *lcd1-1* cannot be determined with this method. However, as there were no significant differences in the amount of cDNA fragment amplified using LCD1 gene-specific primers, it is concluded that the LCD1 mRNA expression level is similar in leaves of the wild type and *lcd1-1*, indicating that the truncation of the last amino acid glutamine does not affect LCD1 mRNA stability. Point mutations present in exons have been reported not to effect the mRNA expression level (Carlson *et al.*, 2000; Conklin *et al.*, 1999). In contrast, mutations in the promoter or in 5'- or 3'-UTR elements have been shown to decrease mRNA stability (Fargo *et al.*, 2000). Thus, post-translational processes, such as protein targeting or folding, may be impaired in the mutant, resulting in loss or decreased function of LCD1. We are currently conducting experiments

to determine whether LCD1 is tissue- or age-specifically expressed, and if it is regulated by light or ROS.

It is worthy to note that a very similar mutant, *rcd2*, has been isolated by Kangasjärvi and colleagues (Kollist *et al.*, 2002). Kollist *et al.* observed that when grown under moderate light, leaves of *rcd2* show the characteristic interveinal paleness of *lcd1-1*. The RCD2 gene was reported to map at 71 ± 2 cM at the bottom of chromosome 2 (Kollist *et al.*, 2002). The mutant has a point mutation in the penultimate intron of the LCD1 gene, indicating that RCD2 is allelic to LCD1 (Kollist, personal communication).

In conclusion, the newly identified LCD1 protein, whose function remains to be determined, may aid in a better understanding of leaf development. It may also help us to better understand the complex network of signal transduction, when plants encounter ROS-generating stress conditions.

Experimental procedures

Plant material and growth conditions

The *lcd1-1* mutant was obtained by mutagenizing the wild-type *A. thaliana* L. Heynh. (ecotype Columbia, Col-0) seed with EMS, as described by Barczak *et al.* (1995). Mutants were screened for ozone sensitivity by ozone fumigation as reported by Conklin *et al.* (1996). For physiological experiments and complementation analysis, 5-week-old F₃ plants from a back-cross between Col-0 wild type and *lcd1-1* were used. Plants used for microscopy were 14 days old. Plants were grown in 15-cm square or in 8-cm round pots in 'Cornell Mix' soil (Landry *et al.*, 1995) in a light room at a PAR of 90–120 $\mu\text{mol photons m}^{-2} \text{sec}^{-1}$ provided by 400 W metal halide bulbs. Plants were grown under a 16-h photoperiod. Temperature in the light room was 21°C and relative humidity was 50%.

Confocal laser scanning and multiphoton microscopy

Confocal and multiphoton images of 2-week-old wild-type and *lcd1-1* plants were taken with an inverted MRC1024 confocal microscope (Bio-Rad, Hercules, CA, USA). Fluorescence was excited at 647 nm for confocal microscopy and at 730 nm for multiphoton microscopy, using an argon-krypton laser and a Ti:Sapphire laser (Tsunami, Spectra-Physics, Mountain View, CA, USA), respectively. For confocal microscopy, fluorescence was detected with a red-sensitive photomultiplier tube using a 680/32 emission filter. In case of multiphoton microscopy, blue (380–480 nm filter), green (500–540 nm filter), and red (560–650 nm filter) channels were used for detection, and were merged. To obtain three-dimensional projections of the leaves, z-scans in 3- μm steps were recorded through the first cell layers beneath the epidermis. In all cases, the middle region of the upper side of a leaf or the entire leaf was imaged. One leaf of the first secondary leaf pair was analyzed while the leaf was still attached to the plant. A 40 \times 1.15 N.A. water objective (Olympus, Melville, NY, USA) was used for imaging. The z-scans were projected by using the software Confocal Assistant 4.02. To stain cell walls in leaf tissue, a 0.1% solution of calcofluor white (Sigma, St. Louis, MO, USA) was infiltrated into detached leaves using a syringe. When roots and early developmental stages were imaged, seeds were germinated

on wet filter paper. For analyzing floral organs, fully developed flowers of both genotypes were used. For seed analysis, dry seeds were placed directly onto the cover glass and were imaged.

Gas-exchange measurements

Plants used for gas-exchange measurements were pre-darkened overnight. Leaves of 5-week-old wild-type and *lcd1-1* mutant plants were enclosed into a cuvette of an infrared gas-exchange system to measure steady-state photosynthesis. The composition of the gas mixture was 0.79 l l⁻¹ N₂, 360 µl l⁻¹ CO₂, and 0.21 l l⁻¹ O₂. CO₂ exchange, transpirational water loss, and conductivity were measured with a LI-6400 portable photosynthesis system (Lincoln, NE, USA). To measure CO₂ assimilation rate as a function of irradiance, the internal light source was used to provide 50, 100, 200, 400, 600, and 800 µmol photons m⁻² sec⁻¹ PAR. For the measurements, a program was designed to perform the gas-exchange analysis, automatically beginning with the highest light intensity. Individual light intensities were applied for 20 min. In the end of the measurements, dark respiration was recorded for 15 min.

Photoinhibition experiments and determination of photosystem I and II activities

For short-term photoinhibition experiments, plants grown for 5 weeks in a greenhouse at 80–100 µmol photons m⁻² sec⁻¹ PAR were pre-darkened overnight for approximately 16 h. Leaf discs 1 cm in diameter were exposed to 2000 µmol photons m⁻² sec⁻¹ PAR at 20 and at 8°C for 90 min as described by Barth and Krause (1999). At the times indicated in the graphs, discs were taken to determine PSI and PSII activities as well as for chloroplast pigment analysis.

As a measure of potential PSII efficiency, the ratio of variable to maximum chlorophyll *a* fluorescence (F_v/F_M) was used. F_v/F_M ratios were measured after 10-min dark-adaptation as described by Barth and Krause (1999). Immediately after potential PSII efficiency was measured, PSI activity was determined by means of P700 absorbance changes measured at 810 nm in the reflectance mode (Klughammer and Schreiber, 1998). Measurements were performed according to Barth and Krause (2002), with the exception that samples were pre-illuminated with 120 µmol m⁻² sec⁻¹ actinic white light for 5 min before applying far-red irradiation to measure P700 absorbance changes.

Chloroplast pigment analysis

Chloroplast pigments were analyzed as described by Barth *et al.* (2001).

Infection of plants with virulent *Pseudomonas syringae* pv. *maculicola* ES4326

The bacterial strain *P. syringae* pv. *maculicola* ES4326 has been described previously by Dong *et al.* (1991). Bacteria were grown to a mid-log phase at 28.5°C in King's B media (King *et al.*, 1954) in the presence of 100 µg ml⁻¹ streptomycin. Prior to infiltration, bacteria were re-suspended in 10 mM MgCl₂ to an inoculation titer of either 10⁶ CFU ml⁻¹ for disease symptom development or to a titer of 10⁵ CFU ml⁻¹ for recording bacterial growth in infected leaves. Plants for infection were germinated in a light room for 2 weeks and then grown for 3 weeks in a controlled environment growth chamber (Western Environmental). Conditions in the growth chamber were: 120 µmol photons m⁻² sec⁻¹ PAR, 8-h photoperiod, 21°C, 70% relative humidity. Inoculation of leaves and

determination of bacterial growth in infected leaves were performed according to Dong *et al.* (1991). In addition, leaf tissue was collected for Western blot analysis.

Protein extraction and Western blot analysis

All samples for Western blot analysis (between 30 and 100 mg) were extracted in 1× Tris buffered saline (0.02 M Tris-HCl, pH 7.4, 0.15 M NaCl), containing 1 mM phenylmethylsulfonyl fluoride, 1 mM benzamide, and 5 mM ε-amino caproic acid. Samples were centrifuged for 5 min at 10 000 g. Protein concentrations were adjusted to 10 µg total protein. Proteins were separated on 15% polyacrylamide gels and transferred to nitrocellulose membranes (Gelman Sciences, Ann Arbor, MI, USA). Before blocking in 5% milk, membranes were stained with Ponceau Red to check equal loading. Membranes were incubated with polyclonal PR-1 and PR-5 antibody, respectively, followed by antirabbit antibody conjugated horseradish peroxidase (Promega, Madison, WI, USA). Blots were developed by using the ECL detection kit from Roche (Indianapolis, IN, USA).

LCD1 locus mapping

The *LCD1* locus was mapped onto the *Arabidopsis* genome with 2090 individuals from a polymorphic F₂-mapping population. This mapping population was generated by self-pollination of F₁ seed from a cross between *LCD1/LCD1* (*Ler* ecotype) and *lcd1-1/lcd1-1* (Col-0 in background). Mutant plants of *lcd1-1* were identified by their characteristic pale phenotype. The initial mapping was accomplished using simple SSLP (Bell and Ecker, 1994) and cleaved amplified polymorphic sequence markers (CAPS; Konieczny and Ausubel, 1993). To create new mapping markers, the Cereon *Arabidopsis* polymorphism collection generated by Cereon Genomics was used (<http://www.arabidopsis.org/Cereon/index.html>). The primer sequences used to amplify the InDels that narrowed down the *LCD1* gene to a 19-kb region on BAC T8P21 are: 5'-AATAATTTGCTCGGCTTCCTCAG-3' (CER447787-5'), 5'-AATCG-GTCCCATGGTCGTTCTA-3' (CER447787-3'), 5'-TTGGCGGATGG-TCTGAATAGTGTC-3' (CER461232-5'), and 5'-TTTTGCTTGGCGCTT-GCTTTTTA-3' (CER461232-3'). To isolate DNA from individual *lcd1-1* mutants, one leaf of 14-day-old plants was ground in 100 µl Tris-EDTA buffer (pH 7.4). One microliter of these homogenates was used and applied to 10 µl GeneReleaser (Bioventure Inc., Murfreesboro, TN, USA) in a polymerase chain reaction (PCR). PCR products were separated by agarose gel electrophoresis and visualized by ethidium bromide staining.

Complementation analysis

A 5.4-kb *EcoRV* fragment containing the ORFs T8P21.22, T8P21.23, and the 3'-half of the ORF T8P21.24, as well as a 4.0-kb *SpeI* fragment containing ORF T8P21.23, were subcloned from BAC T8P21 (obtained from The Arabidopsis Biological Resource Center (ABRC)) and ligated into the binary vector pGreenII0229/*EcoRV* and pGreenII0229/*SpeI*, respectively (http://www.pgreen.ac.uk/a_cst_fr.htm). These constructs were transformed into *A. tumefaciens* (strain LBA4404) by electroporation and introduced into *lcd1-1* plants by the floral dip method (Clough and Bent, 1998). T₁ transformants were selected by their glufosinate-ammonium resistance by sowing seeds and spraying the soil surface with 500 ml m⁻² of 0.25 mg ml⁻¹ commercially available glufosinate/ammonium (FINALE; AgrEvo, Montvale, NJ, USA). Tissue was collected from 4-week-old T₁ transgenic individuals with a wild-type phenotype, and genomic DNA was isolated to check for the presence of the *Bar*

gene by PCR. To determine whether *lcd1-1* lines transformed with a genomic copy of the *LCD1* locus also complement *lcd1-1*-related phenotypes, plants from several complemented lines were fumigated with ozone and infected with virulent *P. syringae* ES4326 as described above.

Genomic DNA, cDNA and sequence analyses

To confirm the public domain sequence of BAC T8P21 that contained the base mutation in *lcd1-1*, both strands of the portion of the wild-type *EcoRV* genomic clone (see above), containing *LCD1*, were sequenced. The *lcd1-1* mutant allele was sequenced from PCR amplification products of genomic DNA. The cDNA encoding the *Arabidopsis LCD1* gene (clone name OBO239, GenBank accession no. F19753 and OBO254, GenBank accession no. F19749) was obtained from Dr Lechary (CNRS, Laboratoire de Biologie du développement des plantes, Institut de Biotechnologie des Plantes, Orsay, France). The OBO cDNA clones were confirmed by sequencing cDNA products amplified from Col-0 wild-type and *lcd1-1* total RNA using the primer 5'-AGTGGCCTAATCACTCTTG-CAGTC-3' in the 5'-UTR and 5'-CAACATTCGAGCTGAAAATTC-3' in the 3'-UTR of the *LCD1* locus. The presence of an 94-bp intron between exon 5 and 6 was furthermore demonstrated by amplification of a cDNA fragment from the wild-type and *lcd1-1* total RNA using the primers 5'-CAGGGCTTCTGGGTTTGCTAT-3' and 5'-TGCCCAATCCAAACTGC-3'. The resulting RT-PCR product was 701 bp in length.

Total RNA extraction and *LCD1* expression analysis by competitive RT-PCR

Total RNA was extracted from leaves of 5–6-week-old plants (approximately 50 mg per extraction) using Tri-Reagent (Molecular Research Center, Inc., Cincinnati, OH, USA), following the manufacturer's protocol. Competitive PCR for quantification of an *LCD1* cDNA fragment was performed according to Gilliland *et al.* (1990), using the Access RT-PCR System (Promega Corporation, Madison, WI, USA). Gene-specific primers were designed based on the published sequence for *LCD1* (At2g37860). These gene-specific primers, 5'-GTTGAGCGGAAAATCTACATC-3' and 5'-CAGGGCTTCTGGGTTTGCTAT-3', gave a 544-bp product when genomic DNA was amplified and a 357-bp product when cDNA was amplified. The reverse transcriptase reaction was performed with 1- μ g total RNA as a starting material. Each PCR reaction contained equal aliquots of the RT reaction and of a dilution series of Col-0 wild-type genomic DNA (ranging from 0.1 to 1 ng μ l⁻¹) that served as the competitor. Aliquots of RT-PCR reactions were diluted 1 : 3 with distilled water and loaded on 1% agarose gels containing ethidium bromide. Band intensities were quantified with ImageQuant 5.0. Experiments were repeated at least three times for each genotype using RNA isolated from different individual plants.

Acknowledgements

We thank Prof. G. Heinrich Krause and Maria Graf (Heinrich Heine University, Düsseldorf, Germany), Jonas Korlach (Developmental Resource for Biophysical Imaging Opto-Electronics (NIH P41-2RR04224), Cornell University, Ithaca, NY, USA), Dr Alain Lechary (Institut de Biotechnologie des Plantes, CNRS, Université de Paris, France), Dr Michael Robinson (USDA-ARS, Beltsville, MD, USA), and David Stern, Dr Greg Martin, Elizabeth H. Williams, and Paul King (Boyce Thompson Institute) for their invaluable assistance in this research. This work was supported by the German Academic

Exchange Service (postdoctoral fellowship D/00/22216 to C.B.) and by the US Department of Agriculture National Research Initiative Competitive Grants Program (Grant no. 96-35100-3212 to P.L.C.).

References

- Aro, E.M., McCaffery, S. and Anderson, J.M. (1993) Photoinhibition and D1 protein-degradation in peas acclimated to different growth irradiances. *Plant Physiol.* **103**, 835–843.
- Asada, K. (1994) Production and action of active oxygen species in photosynthetic tissue. In *Causes of Photo-oxidative Stress and Amelioration of Defense Systems in Plants* (Foyer, C.H. and Mullineaux, P.M., eds). Boca Raton: CRC Press, pp. 77–104.
- Asada, K. (1999) The water-water cycle in chloroplasts: scavenging of active oxygen and dissipation of excess photons. *Annu. Rev. Plant Physiol. Plant Mol. Biol.* **50**, 601–639.
- Barczak, A.J., Zhao, J., Pruitt, K.D. and Last, R.L. (1995) 5-Fluor-oindole resistance identifies tryptophan synthase beta subunit mutants in *Arabidopsis thaliana*. *Genetics*, **140**, 303–313.
- Barth, C. and Krause, G.H. (1999) Inhibition of photosystems I and II in chilling-sensitive and chilling-tolerant plants under light and low temperature stress. *Z. Naturforsch. C*, **54**, 645–657.
- Barth, C. and Krause, G.H. (2002) Study of tobacco transformants to assess the role of chloroplastic NAD (P) H dehydrogenase in photoprotection of photosystems I and II. *Planta*, **216**, 273–279.
- Barth, C., Krause, G.H. and Winter, K. (2001) Responses of photosystem I compared with photosystem II to high-light stress in tropical shade and sun leaves. *Plant Cell Environ.* **24**, 163–176.
- Bell, C.J. and Ecker, J.R. (1994) Assignment of 30 microsatellite loci to the linkage map of *Arabidopsis*. *Genomics*, **19**, 137–144.
- Carlson, S.J., Shanker, S. and Chourey, P.S. (2000) A point mutation at the Miniature1 seed locus reduces levels of the encoded protein, but not its mRNA, in maize. *Mol. Gen. Genet.* **263**, 367–373.
- Clough, S.J. and Bent, A.F. (1998) Floral dip: a simplified method for *Agrobacterium*-mediated transformation of *Arabidopsis thaliana*. *Plant J.* **16**, 735–743.
- Codgell, R.J. and Frank, H.A. (1987) How carotenoids function in photosynthetic bacteria. *Biochim. Biophys. Acta*, **895**, 63–79.
- Conklin, P.L., Williams, E.H. and Last, R.L. (1996) Environmental stress sensitivity of an ascorbic acid-deficient *Arabidopsis* mutant. *Proc. Natl. Acad. Sci. USA*, **93**, 9970–9974.
- Conklin, P.L., Norris, S.R., Wheeler, G.L., Williams, E.H., Smirnov, N. and Last, R.L. (1999) Genetic evidence for the role of GDP-mannose in plant ascorbic acid (vitamin C) biosynthesis. *Proc. Natl. Acad. Sci. USA*, **96**, 4198–4203.
- Demmig-Adams, B. (1990) Carotenoids and photoprotection in plants – a role for the xanthophyll zeaxanthin. *Biochim. Biophys. Acta*, **1020**, 1–24.
- Dong, X., Mindrinos, M., Davis, K.R. and Ausubel, F.M. (1991) Induction of *Arabidopsis* defense genes by virulent and avirulent *Pseudomonas syringae* strains and by a cloned avirulence gene. *Plant Cell*, **3**, 61–72.
- Eskling, M., Arvidsson, P.O. and Akerlund, H.E. (1997) The xanthophyll cycle, its regulation and components. *Physiol. Plant.* **100**, 806–816.
- Fargo, D.C., Hu, E., Boynton, J.E. and Gillham, N.W. (2000) Mutations that alter the higher-order structure of its 5'-untranslated region affect the stability of chloroplast rps7 mRNA. *Mol. Gen. Genet.* **264**, 291–299.
- Gary, R. and Bretscher, A. (1995) Ezrin self-association involves binding of an N-terminal domain to a normally masked C-terminal domain that includes the F-actin binding site. *Mol. Biol. Cell*, **6**, 1061–1075.

- Gilliland, G., Perrin, S., Blanchard, K. and Bunn, H.F. (1990) Analysis of cytokine mRNA and DNA: detection and quantitation by competitive polymerase chain reaction. *Proc. Natl. Acad. Sci. USA*, **87**, 2725–2729.
- Greene, R. (2002) Oxidative stress and acclimation mechanisms in plants. In *The Arabidopsis Book* (Somerville, C.R. and Meyerowitz, E.M., eds). Rockville: American Society of Plant Biologists, pp. 1–19.
- Halliwell, B. and Gutteridge, J.M.C. (1989) *Free Radicals in Biology and Medicine*. Oxford: Clarendon Press.
- Havaux, M., Bonfils, J.P., Lutz, C. and Niyogi, K.K. (2000) Photodamage of the photosynthetic apparatus and its dependence on the leaf developmental stage in the *npq1* *Arabidopsis* mutant deficient in the xanthophyll cycle enzyme violaxanthin de-epoxidase. *Plant Physiol.* **124**, 273–284.
- Huner, N.P.A., Maxwell, D.P., Gray, G.R., Savitch, L.V., Laudenbach, D.E. and Falk, S. (1995) Photosynthetic response to light and temperature – PSII excitation pressure and redox signaling. *Acta Physiol. Plant.* **17**, 167–176.
- Katagiri, F., Thilmony, R. and He, S.Y. (2002) The *Arabidopsis thaliana*–*Pseudomonas syringae* interaction. In *The Arabidopsis Book* (Somerville, C.R. and Meyerowitz, E.M., eds). Rockville: American Society of Plant Biologists, pp. 1–39.
- Kim, G.T., Tsukaya, H. and Uchimiya, H. (1998) The *CURLY LEAF* gene controls both division and elongation of cells during the expansion of the leaf blade in *Arabidopsis thaliana*. *Planta*, **206**, 175–183.
- King, E.O., Ward, M.K. and Raney, D.E. (1954) Two simple media for the demonstration of phycocyanin and fluorescein. *J. Lab. Clin. Med.* **44**, 301–307.
- Klughammer, C. and Schreiber, U. (1998) Measuring P700 absorbance changes in the near infrared spectral region with a dual wavelength pulse modulation system. In *Photosynthesis: Mechanisms and Effects* (Garab, G., ed.). Dordrecht: Kluwer, pp. 4357–4360.
- Kollist, H., Overmyer, K., Tuominen, H., Keinaenen, M. and Kangasjarvi, J. (2002) *Mapping and Characterization of Arabidopsis Light and Ozone-sensitive Mutant, rcd2* (8–20). XIII. International Conference on Arabidopsis Research, <http://www.arabidopsis2002.com/>.
- Konieczny, A. and Ausubel, F.M. (1993) A procedure for mapping *Arabidopsis* mutations using co-dominant ecotype-specific PCR-based markers. *Plant J.* **4**, 403–410.
- Krause, G.H. (1988) Photoinhibition of photosynthesis – an evaluation of damaging and protective mechanisms. *Physiol. Plant.* **74**, 566–574.
- Krause, G.H. (1994) Photoinhibition at low temperature. In *Photoinhibition of Photosynthesis. From Molecular Mechanisms to the Field*. (Baker, N.R. and Bowyer, J.R., eds). Oxford: BIOS Scientific Publishers, pp. 331–348.
- Krause, G.H., Virgo, A. and Winter, K. (1995) High susceptibility to photoinhibition of young leaves of tropical forest trees. *Planta*, **197**, 583–591.
- Krause, G.H., Schmude, C., Garden, H., Koroleva, O.Y. and Winter, K. (1999) Effects of solar ultraviolet radiation on the potential efficiency of photosystem II in leaves of tropical plants. *Plant Physiol.* **121**, 1349–1358.
- Landry, L.G., Chapple, C.C. and Last, R.L. (1995) *Arabidopsis* mutants lacking phenolic sunscreens exhibit enhanced ultraviolet-B injury and oxidative damage. *Plant Physiol.* **109**, 1159–1166.
- Levine, A., Tenhaken, R., Dixon, R. and Lamb, C. (1994) H₂O₂ from the oxidative burst orchestrates the plant hypersensitive disease resistance response. *Cell*, **79**, 583–593.
- Long, S.P., Humphries, S. and Falkowski, P.G. (1994) Photoinhibition of photosynthesis in nature. *Annu. Rev. Plant Physiol. Plant Mol. Biol.* **45**, 633–662.
- Mudd, J. (1997) Biochemical basis for the toxicity of ozone. In *Plant Response to Air Pollution* (Yunus, M. and Iqbal, M., eds). New York: Wiley, pp. 267–284.
- Overmyer, K., Tuominen, H., Kettunen, R., Betz, C., Langebartels, C., Sandermann, H., Jr and Kangasjarvi, J. (2000) Ozone-sensitive *Arabidopsis rcd1* mutant reveals opposite roles for ethylene and jasmonate signaling pathways in regulating superoxide-dependent cell death. *Plant Cell*, **12**, 1849–1862.
- Padh, H. (1990) Cellular functions of ascorbic acid. *Biochem. Cell Biol.* **68**, 1166–1173.
- Powles, S.B. (1984) Photoinhibition of photosynthesis induced by visible light. *Annu. Rev. Plant Physiol. Plant Mol. Biol.* **35**, 15–44.
- Rao, M.V. and Davis, K.R. (1999) Ozone-induced cell death occurs via two distinct mechanisms in *Arabidopsis*: the role of salicylic acid. *Plant J.* **17**, 603–614.
- Rao, M.V., Koch, J.R. and Davis, K.R. (2000) Ozone: a tool for probing programmed cell death in plants. *Plant Mol. Biol.* **44**, 345–358.
- Schraudner, M., Moeder, W., Wiese, C., Van Camp, W., Inzé, D., Langebartels, C. and Sandermann, H., Jr (1998) Ozone-induced oxidative burst in the ozone biomonitor plant, tobacco Bel W3. *Plant J.* **16**, 235–245.
- Sonoike, K. (1996) Photoinhibition of photosystem I: its physiological significance in the chilling sensitivity of plants. *Plant Cell Physiol.* **37**, 239–247.
- Tenhaken, R., Levine, A., Brisson, L.F., Dixon, R.A. and Lamb, C. (1995) Function of the oxidative burst in hypersensitive disease resistance. *Proc. Natl. Acad. Sci. USA*, **92**, 4158–4163.
- Thiele, A., Winter, K. and Krause, G.H. (1997) Low inactivation of D1 protein of photosystem II in young canopy leaves of *Anacardium excelsum* under high-light stress. *J. Plant Physiol.* **151**, 286–292.
- Tjus, S.E., Scheller, H.V., Andersson, B. and Moller, B.L. (2001) Active oxygen produced during selective excitation of photosystem I is damaging not only to photosystem I, but also to photosystem II. *Plant Physiol.* **125**, 2007–2015.
- Tsukaya, H. (2002) Leaf Development. In *The Arabidopsis Book* (Somerville, C.R. and Meyerowitz, E.M., eds). Rockville: American Society of Plant Biologists, pp. 1–19.
- Van Loon, L.C. (1997) Induced resistance in plants and the role of pathogenesis-related proteins. *Eur. J. Plant Path.* **103** (9), 753–765.
- Xie, Z., Ho, W.T. and Exton, J.H. (2000) Conserved amino acids at the C-terminus of rat phospholipase D1 are essential for enzymatic activity. *Eur. J. Biochem.* **267**, 7138–7146.

Arabidopsis seed stock: CS6359 F4 BC3 Col × soz2.